

An Optimization Framework for Joint Sensor Deployment, Link Scheduling and Routing in Underwater Sensor Networks

L. Badia
IMT Lucca Institute for
Advanced Studies
Lucca, Italy
lbadia@ing.unife.it

M. Mastrogiovanni,
C. Petrioli, S. Stefanakos
Department of Computer
Science
University of Rome "La
Sapienza"
Rome, Italy

M. Zorzi
Department of Information
Engineering
University of Padova
Padova, Italy
zorzi@ing.unife.it

mastrogiovanni@di.uniroma1.it

ABSTRACT

Underwater sensor networks are a very interesting case of wireless communication in extreme conditions. They exploit acoustic communication in sea water and are nowadays used in surveillance and monitoring applications. These networks present very challenging aspects, such as low data rates and large delays, as well as the special propagation characteristics of the underwater medium. We propose an integer-linear programming approach to jointly optimize routing, link-scheduling and node placement in such a scenario. Accounting for these special aspects of underwater wireless communications leads to re-thinking traditional approaches; this results in original solutions, which highlight novel directions for further research in this area.

Categories and Subject Descriptors

C.2.2 [Computer Systems Organization]: Computer-Communication Networks—*Network Protocols*

General Terms

Algorithms

Keywords

Underwater sensor networks, Acoustic communications, Routing, Scheduling, Energy efficient protocols

1. INTRODUCTION

Underwater (UW) sensor networks are an emerging topic of research, coupling interesting application scenarios with very challenging technical issues [1, 18]. The features of acoustic waves, which are the wireless communications technology of choice in underwater networks, are so different from their RF counterpart that the (by now well established) algorithms and models that were proposed in

the past few years for wireless sensor networks [17, 20] are not suitable for this new environment, and cannot be applied to it without significant modifications or even a completely new design. One of the main applications of underwater sensor networks is the surveillance and monitoring of sea areas. Oceanic monitoring is used to detect tectonic movements, incoming tsunamis, water pollution, global warming, and many other facts that are bound to affect our lives. Sensor networks for underwater monitoring can consist of water column and/or seafloor sensors, possibly connected to moored buoys providing connectivity back to the land. In general, these sensors are expensive and therefore we expect to have networks formed by a limited number of nodes, whose performance has to be optimized in order to justify the high deployment costs.

The typical physical layer technology for underwater wireless sensor networks is acoustic communication. Acoustic waves travel in a way that depends on the properties of the medium (i.e., the sea water). Unique features of underwater sensor networks resulting from the use of acoustic communications include low data rates, high error rates, and large propagation delays, making them related to delay-tolerant networks [2]. In studying routing and link scheduling problems in such networks, models of static flows, i.e., with zero link-transit times and fixed capacity, which are usually employed for terrestrial wireless networks, become inadequate. Thus, we need to employ new models and algorithms, e.g., dynamic network flow models [11], since link-transit times in the underwater scenario are considerably large and can not be ignored as is usually done in terrestrial radio communications. In this paper, we consider a scenario where a sink node is in charge of collecting all the information coming from the sensors [13, 21]. We propose an optimization model which jointly addresses both routing and link-scheduling. We also assume that additional nodes can be placed in order to relay the flows from the traffic-generating sensors to the sink, which adds another degree of freedom in order to improve the efficiency of the solution.

In general, determining a feasible routing scheme together with choices of powers, rates and overall transmission schedule, is an interesting and challenging problem for wireless networks [9, 12]. In underwater scenarios, this is even more difficult because of the more stringent delay and interference constraints. We aim at energy efficiency, which is frequently taken as a goal for wireless networks [3, 13, 17]. In underwater scenarios, having low energy consumption is even more important since battery replacement or re-charge for the sensors is very difficult. We therefore assume that minimizing the energy consumption is the objective of our optimization, similarly to [4, 15]. However, the interference model in these papers is usually treated with drastically simplified approaches, which might be

Permission to make digital or hard copies of all or part of this work for personal or classroom use is granted without fee provided that copies are not made or distributed for profit or commercial advantage and that copies bear this notice and the full citation on the first page. To copy otherwise, to republish, to post on servers or to redistribute to lists, requires prior specific permission and/or a fee.

WUWNet'06, September 25, 2006, Los Angeles, California, USA.
Copyright 2006 ACM 1-59593-484-7/06/0009 ...\$5.00.

a problem when multiple parallel transmissions are coordinated in a critical environment such as underwater networks. We aim at improving also this point by taking more realistic interference aspects into considerations.

The original contribution of our analysis is the availability of optimality results, which can be used to implement practical joint strategies for routing, scheduling and node placement in relatively small underwater networks. Note that typical underwater network deployment are not as densely populated as terrestrial wireless sensor networks. For example, past projects dealing with the development of underwater monitoring systems, such as the Seaweb network for FRONT Oceanographic Sensors [5], report the deployment of no more than 10-20 nodes. We therefore expect that our approach is suitable also for network design in realistic cases.

The rest of this paper is organized as follows: in Section 2 we outline the unique characteristics of the underwater scenario in terms of propagation of the acoustic waves. In Section 3 we present our network model. In Section 4 we formulate the optimization problem as an Integer Linear Program (ILP) and discuss how we can iteratively solve this and augment it with new constraints in order to properly model the effect of physical interference. Finally, in Section 5 we present some performance evaluation results and in Section 6 we conclude.

2. UW PROPAGATION MODEL

Usually, optimization frameworks for wireless networks are applied on a graph representation of the network, obtained based on simple assumptions about propagation. However, the attenuation of transmitted signal power undersea does not match the most common models of RF propagation. For this reason, the derivation of the network topology for underwater scenarios is itself a challenging issue. Indeed, accurate evaluations of underwater propagation would require massive amounts of measurements. Moreover, usual models for acoustic attenuation refer to a single transmitter-receiver pair, and are not designed to be employed in a network scenario where different links coexist.

In order to obtain a viable but realistic model, able to derive the network topology while at the same time capturing the special characteristics of the underwater medium and therefore their impact on the schedule design, we propose in this section a path loss model description, obtained by directly applying underwater acoustic physics in order to capture the most relevant propagation phenomena. The model can be seen as an extension of what reported in [19, pages 174–181], following the same line of thought but aiming at a more accurate description for what concerns networking applications (in particular, co-existing links and interference evaluation).

In underwater propagation, at close distances from the transmitter the acoustic energy spreads according to a spherical geometry. When the distance is very large, the spreading area becomes cylindrical. In between, there is a transition region with hybrid propagation between spherical and cylindrical spreading.

Let us focus for the moment on horizontal propagation paths. For these links, we can describe the transitions of the geometry of the spreading area following [19], where this aspect of the propagation scenario is described by means of a *characteristic length* H , which is a value assigned a priori for the scenario. The physical meaning of H is that the propagation is well modeled as spherical or cylindrical for distances lower than H or higher than $10H$, respectively, whereas in between it exhibits a hybrid behavior. For deep water scenarios, H is very high (this practically means that the propagation is always spherical). For shallow water scenarios, H is empirically set: a rough estimate of H can be obtained by dividing the water depth by 2. In general, the deeper the water, the higher H . For non-horizontal

links, the reasoning of [19] can be repeated by considering the projection of the link on a horizontal plane. Note that, whereas [19] only considers single links, we are interested in comparing all the links present in the network, which have different propagation angles. For this reason, we need to extend the formulae of [19] by also adding the propagation angle ϑ between the horizontal plane and the propagation direction.

In addition to the propagation geometry, other factors impact on the path loss. Spreading of the sonic waves is not the only cause of sound attenuation, there is also absorption by the medium, generally modeled with an additional loss which is exponential in linear scale. Finally, an additional term called transmission loss anomaly is introduced to take into account other factors such as variations from the theoretical model depending on water temperature, salinity, sea conditions and so on.

To sum up, the path loss $G(d)$ between an underwater acoustic transmitter and receiver placed d meters apart is

$$G(d) = AS(d)e^{-\alpha d} \quad (1)$$

where A is the transmission anomaly, α is an absorption coefficient and $S(d)$ is the spreading loss. In the following, we will set $\alpha = 2 \cdot 10^{-4} \text{m}^{-1}$, which gives approximately an attenuation factor of 1 dB per kilometer. The transmission anomaly term A has been set equal to 1 for simplicity (indeed, this choice is not very relevant in practice since the system is interference limited and therefore the path losses mostly intervene in the optimization through ratios). These choices simply follow from the application of classic underwater propagation models to typical scenarios [19].

In this paper, we propose some modifications to the path loss term $S(d)$, in order to better capture networking issues. To model the aforementioned geometrical aspects, $S(d)$ should decrease proportionally to d^{-2} for the case of spherical spreading and d^{-1} when the spreading area is cylindrical. In the intermediate region, [19] proposes a behavior proportional to $d^{-1.5}$. This is a purely heuristic choice, which might not be good for our purposes, since when comparing multiple links the transition between spreading modalities should be as smooth as possible. For this reason, we propose an alternative formula, which gives a continuous first derivative to $S(d)$ (which means a smoother behavior) as a function of d . Specifically, we take $S(d)$ as equal to

$$\begin{cases} d^{-2} & \text{if } d \cos \vartheta \leq H \\ d^{-2} (d \cos \vartheta / H)^{(\log_{10}(d \cos \vartheta / H))/2} & \text{if } H < d \cos \vartheta \leq 10H \\ d^{-1} H^{-1} \cos \vartheta \sqrt{0.1} & \text{if } d \cos \vartheta > 10H. \end{cases} \quad (2)$$

The definition of $S(d)$ fully specifies the path loss model. This can be used to evaluate where to place the sensors in the network, as well as how to establish the links, over which routing and scheduling will be determined. These tasks will be performed through the optimization framework introduced and solved in the following.

Finally, links delay is another propagation aspect which needs to be carefully accounted for in underwater scenarios. In general, we should consider that speed of sound underwater is affected by pressure and temperature changes [19]. In this paper we neglect these effects and adopt a simpler approach, where sound speed is considered constant. We set the sound speed to 1531 m/s and calculate all delays accordingly. Note that we could have evaluated link delays via a more elaborate approach: no change in the model is needed provided that delays can be set a priori for all links. Note also that the impact of the variability of the sound speed in the considered scenario (we consider links which span a few hundreds meters) is very limited.

3. NETWORK MODEL

We model the network via a directed graph $\mathcal{G}(\mathcal{V}, \mathcal{E})$ in a three-dimensional space modeling the sea. The nodes in \mathcal{V} are *candidate* positions, i.e., they represent points in the three-dimensional space, where it is possible to place a sensor. The actual positions of the sensors will be decided by the outcome of the optimization procedure. If we assume that underwater sensors are attached to buoys or placed in grids, it appears reasonable to assume their placement as limited to a discrete number of possible positions.

We assume that certain positions belonging to $\mathcal{S} \subseteq \mathcal{V}$ generate a given amount of data which need to be transmitted to a special node v_t called *network sink*. For this reason, sensors must be mandatorily placed in positions generating data and also in v_t . We assume that the data are grouped into packets of identical size and, for any position $v \in \mathcal{V}$, we denote with s_v the *packet generation rate*, i.e., the number of packets to transmit to the sink in one time period. We can therefore distinguish between positive generation rate positions, where data are generated, and positions with $s_v = 0$, which are only introduced as candidates for relay placement. Finally, v_t has a negative generation rate equal to: $s_{v_t} = -\sum_{v \in \mathcal{V} \setminus \{v_t\}} s_v$.

According to the propagation model defined in Section 2, we can evaluate the path loss between every pair of nodes in \mathcal{V} . From the evaluation of these gains, the edges of \mathcal{E} are derived as follows. We assume that each node can choose among a fixed number of transmit power levels. We denote the set of available power levels by Π . The maximum power level is denoted by π_{\max} . Let $\pi_T(u, v)$ denote the minimum power level required for a reliable transmission from node u to node v . If for simplicity we assume that all nodes are capable to correctly hear a transmission if the received power is above a value π_{\min} , then $\pi_T(u, v) = \pi_{\min}/G(d(u, v))$, where $d(u, v)$ denotes the distance between u and v and $G(\cdot)$ is the underwater propagation gain. In order to allow for the implementation of interference considerations in our model, we add in \mathcal{E} one directed edge e from u to v for each power level $\pi \in \Pi$ with $\pi_T(u, v) \leq \pi \leq \pi_{\max}$. We denote with $\pi(e)$ the power level associated with edge e . We remark that in this way we obtain redundant links between nodes. However, this is intentional, since first of all this way of generating edges allows us to account for a preliminary power control already in the graph topology. Moreover, even though every link between the same transmitter/receiver pair is identical for what concerns routing, it is not for the interference evaluation. This is a very important contribution of our work, which differentiates it from other studies dealing with network topologies modeled as a graph [4, 9]. In general, those studies assume that only one link exists between two nodes and that such link exists iff the transmitter can reach the receiver with at least one power level. However, with this approach only very simplified interference models can be used. This point will be further discussed later in this section when dealing with interference issues.

We denote by $c_{\text{tx}}(e)$ and $c_{\text{rx}}(e)$ the energy costs required for transmitting and receiving a packet on link e , respectively. The cost $c_{\text{tx}}(e)$ should take into account the power required for a reliable transmission over link e , since each link is associated with a certain power level of transmission. We do not include fixed terms for, e.g., the energy required for listening to the channel. One can assume, as in [15], that nodes are synchronized and a node is awake only when it is scheduled to send/receive a packet. In any case, we minimize the energy consumption at each node and these terms would be identical for all nodes. We use $\mathcal{U}^{\text{out}}(v)$ and $\mathcal{U}^{\text{in}}(v)$ to denote the sets of edges directed out of and into node v , respectively. For a directed edge $e = (u, v)$, we say that the transmitter or sender node u is the tail of e while the receiver node v is the head of e . Each edge e in \mathcal{E} is also associated with a propagation delay on the acoustic medium $d(e)$. Since we want to capture interference issues, we need to eval-

uate the delays in the cases in which the transmission is heard also by nodes who are not the intended receivers of that link. For this reason, we need to define delays not only for the edges in \mathcal{E} , but also for every pair of different edges, where the delay $D(f, e)$ between links f and e is actually the delay of the acoustic signal from the tail of link f to the head of link e . Observe that, in general, $D(f, e) \neq D(e, f)$, and in every case in which a link $g \in \mathcal{E}$ exists between the tail of link f and the head of link e , $D(f, e) = d(g)$. In particular, $D(e, e) = d(e)$. We can think of collecting all these delays in an $|\mathcal{E}| \times |\mathcal{E}|$ transmission-delay matrix evaluated a priori.

For the scheduling, we will focus on periodic scheduling of transmissions from the nodes. This is a very easy way to obtain an efficient and scalable schedule, which is assumed to be repeated at every period. Another motivation for this assumption is that sensor traffic for underwater monitoring is expected to be highly periodic. We assume the period consists of T slots, all equal in length. The fundamental period is denoted by the set $\mathcal{T} = \{0, 1, 2, \dots, T-1\}$. Note that time T does not belong to \mathcal{T} , but it corresponds to the first time instant after the end of the period. In one period of time, each node v generates s_v packets and all these packets must be forwarded to the sink before time T . A work hypothesis we have is that all these packets are already available at the beginning of each period. Including also generation of packets *within* a period is a reasonably easy extension of our model which is left for future investigation. Finally, we remark that this way of treating the scheduling problem also gives a certain level of delay guarantee since if a feasible schedule is found, then all packets are surely delivered with a delay lower than T slots. Note that while transmissions occur at the exact time steps $0, 1, \dots, T-1$, receptions can happen at any time. This is an important and necessary feature of our model since links have long delays which might not be integer multiples of the length of the slot.

A very important aspect of our model is that of interference. In the literature, most of the optimality frameworks for scheduling/routing problems focus on the so-called *protocol interference model* [8, 10], which relies on simplified assumptions based on the behavior of the IEEE 802.11 Medium Access Control (MAC). This means that a necessary and sufficient condition for the correct delivery of a packet is that this is the only transmission which takes place in the transmitter's and receiver's radio ranges. Basically, this means that both hidden and exposed terminal problems must be avoided. This leads to developing nice and clean mathematical constraints, which are however not suitable for the underwater scenario, for several reasons. First of all, since we aim at designing an optimized schedule which is inherently collision-free, we do not need collision avoidance mechanisms as per IEEE 802.11 MAC.¹ Moreover, the underwater propagation range can vary widely, as discussed in Section 2, and it is possible that excluding every node in coverage range from transmission would be too restrictive. For example, consider networks where the nodes are very close so to form a clique: the protocol interference model would not allow simultaneous transmissions in this case, even though they might be physically possible, as will be discussed next. Last but not least, the additive character of the interference is completely ignored in this model.

Note that sometimes [8, 16], the protocol interference model is also extended by considering a compatibility graph between links, which interfere with each other in a more general way. However, the relationship is still binary, i.e., the additive behavior of the interference is not considered at all.

In this paper, we aim at improving this description by mixing the formulation of the protocol interference model through compatibility graph and also referring to the concept of *physical interference*

¹Note also that, because of long propagation delays, in our scenario four-way handshaking would lead to sub-optimal performance.

model as described by [7]. We will therefore derive a compatibility relationship through links with a check on the received Signal-to-Interference Ratio (SIR), to see if it is above a given threshold for every received packet. This is complicated in underwater scenarios by the aforementioned property that packets are not received, or perceived as interference by a receiver, at the same time at which they are transmitted.

For the sake of implementation simplicity, we take a two-step approach. First, we impose that for the correct reception at node v from a link e , all other transmissions which might interfere must be silent if they are marked as conflicting with e . This can be expressed as follows. We define the *set of conflicting links* for link e and denote it by $\mathcal{E}_I(e)$; an edge $f = (w, z)$ belongs to the set of conflicting links of $e = (u, v)$ if its activation prevents node v from correctly receiving the packet sent by u , since it causes the transmission made by u to be heard at node v with too low an SIR (i.e., under a given threshold γ_{th}). Note that the interfering link is not necessarily meant to have v as its destination. This means that

$$\mathcal{E}_I(e) = \{f = (w, z) \in \mathcal{E} : \frac{G(d(u, v))\pi(e)}{G(d(w, v))\pi(f) + \eta(e)} < \gamma_{th}\}, \quad (3)$$

where $\eta(e)$ is the ambient noise power at the receiver of link e (in the numerical evaluation it has been set to 1 nW for all links).

The above formulation neglects interference additivity, but is useful in order to simplify the solutions by discarding pairs of links which can not transmit simultaneously. This can be easily included, with the proper timing, in the optimization framework through linear constraints, as will be shown in the following.

After solving the linear program formulated above, we additionally check the SIR at every node for the resulting schedule. If it happens that the SIR is too low for some received packets, e.g., since many far-away nodes are all transmitting simultaneously, we add more constraints to the linear program and look for a new solution. This way to proceed can be seen as a simple manner to introduce more realistic interference characterization, which is required for underwater sensors, without complicating the model too much. The price to pay is that this iterative approach is not optimized for quick evaluations. For this reason, further development of this strategy to improve the integration between the theoretical and practical interference models is surely an interesting aspect for future research. However, we emphasize that if the interference range is carefully chosen, we observe that in practical cases of underwater networks (where the number of nodes and power levels are not very large) additional executions of the optimization program due to interference problem do not occur very often.

4. ILP FORMULATION

In this section we formulate the integer-linear program to solve in order to find optimal node deployment, routing and link scheduling for a given network $\mathcal{G} = (\mathcal{V}, \mathcal{E})$. The key variables of the models are binary values y_v , which indicate whether or not a sensor is actually placed in the candidate position v (which solves the optimal network deployment problem), and $X_e(t)$, which indicate whether the tail of link e is transmitting over e at time t . This completely specifies scheduling and, looking at the whole time period, i.e., taking $t = 0, \dots, T-1$, also routing. We first formulate the basic constraints of the ILP problem subject to flow conservation constraints and the protocol interference model. Secondly, we add interference considerations according to the discussion reported at the end of the previous section.

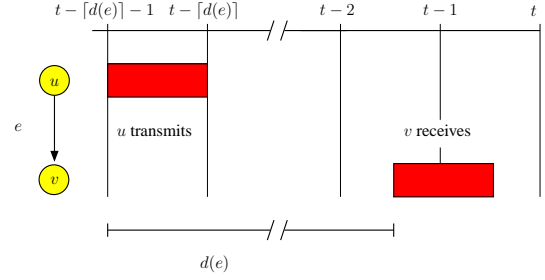


Figure 1: Sending a packet over link $e = (u, v)$: to fully receive it at time t we have to begin transmission at time $t - [d(e)] - 1$.

4.1 Basic Formulation

The following flow conservation constraints ensure that at any time step t before the end of the period the number of messages that have been transmitted from each node v are at most the generation rate of v plus the number of messages that have been received at v till time t .

$$\sum_{e \in \mathcal{U}^{\text{out}}(v)} \sum_{r=0}^t X_e(r) - \sum_{e \in \mathcal{U}^{\text{in}}(v)} \sum_{r=[d(e)]+1}^t X_e(r - [d(e)] - 1) \leq s_v, \quad v \in \mathcal{V}, 0 \leq t < T - 1. \quad (4)$$

Note that the delays of the links are implicitly accounted for in the above constraint (see Fig. 1): the packet that node v receives completely at time t over an incoming link e , is what is being sent at time $t - [d(e)] - 1$ at the other end of the link. Note also that time $t = T - 1$ is excluded in the above constraint, since it refers to the last transmission of the period, for which a stronger constraint holds, as explained below. At time step T , we want to have cleared all traffic from the network so that we can begin with the next period in the schedule. Thus, we require that after the transmissions occurring at time $T - 1$ all the traffic has been delivered to the sink. This is obtained by checking at every node that the total number of outgoing messages minus the total number of incoming messages is equal to the generation rate s_v . Remember that this last value is positive for the data generating positions, zero for the relays and negative for the sink. Thus, we apply the same formulation of Eq. (4), but replacing the inequality with an equality sign.

$$\sum_{e \in \mathcal{U}^{\text{out}}(v)} \sum_{r=0}^{T-1} X_e(r) - \sum_{e \in \mathcal{U}^{\text{in}}(v)} \sum_{r=[d(e)]+1}^{T-1} X_e(r - [d(e)] - 1) = s_v, \quad v \in \mathcal{V}. \quad (5)$$

Note that Eq. (4) holds for $t < T - 1$, whereas Eq.(5) holds at time $T - 1$.

We define a simple Boolean function $B(a, b)$ that is true if and only if $|a - b| < 1$ and false otherwise.

We use this function for checking whether two packets overlap or not. Overlapping of packets happens when they both arrive at the same node v and their arrival times differ less than one slot. More formally, in the case of concurrent reception, for each node v and links $e, f \in \mathcal{N}^{\text{in}}(v)$ overlapping occurs when:

$$X_e(t_e) + X_f(t_f) \leq 1 \quad \Leftrightarrow \quad B(t_e + d(e), t_f + d(f)), \quad (6)$$

where t_e is the transmitting time over link e and t_f is transmitting time over link f .

In case of overlapping transmission and reception we have for each edge $e \in N^{in}(v)$, $f \in N^{out}(v)$:

$$X_e(t_e) + X_f(t_f) \leq 1 \Leftrightarrow B(t_e + d(e), t_f), \quad (7)$$

We even impose that a node cannot transmit over multiplex edges at same time:

$$\forall v \in V, t \in \mathcal{T}, \quad \sum_{e \in N^{out}(v)} X_e(t) \leq 1 \quad (8)$$

We add constraints in the ILP to model the interference as defined in the protocol interference model. For each edge e we denote a set of interferers for link e by $\mathcal{E}_I(e)$; an edge $f = (w, z)$ belongs to the set of interferers of $e = (u, v)$ if its activation prevents node v from correctly receiving the packet sent by u .

The constraint is imposed for every couple of edges $e \in \mathcal{E}$ and f such that $f \in \mathcal{E}_I(e)$:

$$X_e(t_e) + X_f(t_f) \leq 1 \Leftrightarrow B(t_e + d(e), t_f + D(f, e)), \quad (9)$$

The following constraints use the binary variables y_v to check the node placements. To ensure that we place at most k sensors:

$$\sum_{v \in \mathcal{V}} y_v \leq k.$$

Only nodes where sensors are placed can be used for sensing and relaying data. Thus, we require that y_v be equal to 1 if v is used at some time step for transmitting:

$$X_e(t) \leq y_v, \quad v \in \mathcal{V}, e \in \mathcal{U}^{out}(v), t \in \mathcal{T}.$$

(We do not need to force this constraint for incoming edges since besides the sink all other nodes have to transmit if they are used; for the sink, we set $y_{v_t} = 1$ anyway.) Finally, we set $y_v = 1$ for all the sources and the sink and force the y_v variables to be 0-1 variables.

$$\begin{aligned} y_v &= 1, & v &\in \mathcal{S} \cup \{v_t\} \\ y_v &\in \{0, 1\}, & v &\in \mathcal{V}. \end{aligned}$$

Finally, the goal of our optimization problem is to minimize the total energy consumption:

$$\text{minimize } \sum_{e \in \mathcal{E}} \sum_{t=0}^{T-1} X_e(t) (c_{tx}(e) + c_{rx}(e)). \quad (10)$$

4.2 Augmenting the ILP with Physical Interference Constraints

Having obtained a link schedule by solving the ILP formulation described in the previous section, we check the signal-to-interference ratio (SIR) at the receiver of every active link. Whenever this ratio is below some pre-defined threshold, we augment the ILP with extra constraints and solve it again. We need to measure the SIR at every packet reception. Assume that, according to the current link schedule obtained from the ILP, node v is receiving a packet over link $e = (u, v)$ at some time step t . The SIR at the receiver of link e at a generic time t , even between two time steps, i.e., not necessarily integer, but such that $X(\lfloor t - D(e, e) \rfloor - 1) = 1$, is

$$\gamma_e(t) = \frac{G_{e,e} \cdot \pi(e)}{\sum_{f \in \mathcal{E}: f \neq e, X_f(\lfloor t - D(f, e) \rfloor) = 1} G_{f,e} \cdot \pi(f) + \eta(e)}.$$

In the above expression,

- $G_{f,e}$ denotes the gain from the tail of link f transmitting over f to the head of link e and the diagonal entries $G_{e,e}$ represent the gains over each link e ,
- $\pi(e)$ is the transmit power associated with link e ,
- $\eta(e)$ is the ambient noise power at the receiver of link e .

For each link e , we can impose the additional requirement that for all packet receptions the SIR is at least γ_e^{target} . Note that due to the arbitrary link-delay times, measuring the SIR for a single packet reception is not completely straightforward. Several packets might interfere with the packet whose SIR we are measuring, and the interfering packets need not be arriving at the receiver simultaneously. To deal with this increased complexity, we have to measure the SIR more than one time to verify the successful reception of just one packet.

The SIR condition must be in fact verified for every superposition of interfering packets which occurs during the reception of link e . Thus, first of all, we sort the interfering packets in non-decreasing order of arrival. After that, we consider all the time instants where the reception of an interfering packet terminates or starts during the reception of a packet on link e . For these instants, (i.e., immediately before a termination or immediately after a new reception) we measure the SIR $\gamma_e(t)$ as indicated above to evaluate if it is above the given SIR target.

In the case this condition is violated, we have found a set of links \mathcal{I} that interfere with reception at node v . Thus, we augment the original ILP by adding a constraint that ensures that at most $|\mathcal{I}|$ of the links in $\mathcal{I} \cup \{e\}$ can coexist. We then solve again the new ILP and iterate this process until a solution that does not violate the SIR constraint is found or infeasibility is detected.

For what concerns this two-step approach, note the following. First of all, the termination condition is bound to happen in a finite time, so it is guaranteed that either a solution to the original problem is found or infeasibility is detected. Also, observe that this approach still preserves the optimality of the solution, even though the time to find it may not be the shortest. In fact, the augmentation simply discards solutions which are feasible according to the above constraints but still are impossible to realize in practice (due to additive interference). Therefore, the two step procedure is guaranteed to find the optimal solution in the sense of satisfying both the optimization problem and the SIR conditions at every link, and the allocation jointly chosen according to these criteria is the best possible according to the goal function.

5. PERFORMANCE EVALUATION

We have based our evaluations on the parameters of the UWM1000 LinkQuest underwater acoustic modem [14]. The product series of LinkQuest is representative of current underwater acoustic technology. In our experiments sensors are assumed to be equipped with the UWM1000 model, a short range modem designed for being placed at low depths. The specifications indicate that correct functionalities are guaranteed for distances up to 350 m and that sensors equipped with the UWM1000 modem should be placed at a maximum sea depth of a few hundred meters. The achievable data rate is 9600 bps. The modem has two power levels (2 W and 8 W) for transmission and consumes 0.75 W in reception mode. When no data is being sent or received the modem enters a sleep mode with minimal power consumption (8 mW). The modem can successfully receive if the SIR is above $\gamma_e^{\text{target}} = 10$ dB.

In our experiments, the candidate sensor positions \mathcal{V} are arranged according to a 3D grid. The maximum number of sensors that can be deployed is k . A number $|\mathcal{S}|$ of candidate positions are traffic sources, and therefore a sensor must be placed in each of them as

well. Finally, we have the option of placing up to $k - |S|$ additional sensors that, while not generating any traffic, play the role of relays in forwarding packets to the sink. The sink is assumed to be mounted on a buoy floating on the sea surface. We assume a packet size of 2000 bits. Thus, with a data rate of 9600 bps, the length of a time slot is roughly 0.2 s.

The input parameters to be given to our model are: the number of candidate sensor positions, $|\mathcal{V}|$, and their arrangement on a 3D grid; the number $|S|$ and the set of positions S ; the position of the sink; the number of packets generated by each source in each scheduling period, p ; the maximum schedule length T ; and the maximum number of sensors k . Given these parameters the model provides the best placement of the $k - |S|$ relay sensors, and the traffic schedule and routing which minimize the total energy consumption.

A first step in the assessment of our model has been to establish its scalability in realistic underwater sensor network scenarios. For this purpose, we have solved the ILP model for different values of the traffic load, the grid size, the number of sensors k and the schedule length T . The solver we have used is GLPK, version 4.8 [6]. The model was able to find the optimum schedule, node placement and routing in reasonable underwater sensor network scenarios with more than 50 candidate positions, 30 sensors, $T = 40$ slots, and a traffic of up to 25 packets per node per schedule. The number of additional iterations of the program due to the SIR check (as explained in Subsection 4.2) until it found a feasible solution or it detected infeasibility never exceeded 25. The overall model running time in these scenarios was typically around three hours using a Linux PC with 2.8 GHz Intel Xeon processors and 1 GB of RAM, which shows that the model can be applied to realistic underwater sensor networks.

A second step in our evaluation has been to look at the solution provided by our model. The main purpose of our investigation has been to assess the model, and specifically to understand whether it could provide useful insights on effective protocol design criteria for underwater network settings, as well as on the performance that can be expected in these networks.

In the first scenario in which we have tested our optimization framework $|\mathcal{V}| = 19$, and sensor candidate positions are placed in a $3 \times 3 \times 2$ grid. The grid size is approximately $600 \times 600 \times 200$ cubic meters. Nine nodes, placed on the seafloor (at a depth of 200 m), generate traffic. At a depth of 50 m, nine candidate positions (for relay nodes only) are also considered. The number of packets p generated by each source node has been varied between 1 and 2 per scheduling period.

The metrics we have investigated are the following: 1) end-to-end packet latency, defined as the time it takes, on average, from when the packet is generated to when it is successfully delivered to the sink; 2) minimum time T needed to completely deliver all generated packets to the sink; 3) total energy consumption, defined as the total energy consumed by all network nodes in a scheduling period to deliver the $|S| \times p$ packets to the sink. 4) energy efficiency, defined as the average energy needed to successfully deliver a packet to the sink (obtained normalizing the total energy consumption by the number of delivered packets). Results are displayed in Table 1, where each value represents the average over 10 different runs. In each run, an independent random horizontal/vertical offset has been added to each candidate position in \mathcal{V} , to model the fact that actual sensor locations might slightly oscillate around their nominal value due to sea waves and random floating. This offset has been taken as Gaussian distributed with zero mean and a standard deviation equal to 33 and 10 meters for the horizontal and vertical directions, respectively.

For each choice of \mathcal{V} , S , and p , we have solved the model for large T and k , in order to find a feasible minimum-energy solution. To further optimize delay and cost, we have progressively decreased

T and k as long as we could find a feasible solution with the same energy performance. The results shown in the figures correspond to the smallest T and k values able to provide minimum energy consumption.

Total Energy Consumption (J)	p=1	p=2
sink centrally placed	86.5	173
sink placed at the side	107.25	214.5
Energy Efficiency (J)	p=1	p=2
sink centrally placed	9.61	9.61
sink placed at the side	11.92	11.92
End-to-end latency (s)	p=1	p=2
sink centrally placed	9.20	20.96
sink placed at the side	12.47	28.20
Time to deliver all packets to the sink (s)	p=1	p=2
sink centrally placed	3.2	7
sink placed at the side	4	8.8

Table 1: Scheduling and routing performance

Table 1 shows that as the traffic increases the total energy consumption also increases, as one would expect since nodes are involved in transmitting and receiving more packets resulting in an overall higher energy consumption. However, if we look at the energy cost per delivered packet, no degradation is observed as the traffic increases.

In the considered scenario, if there is no interference, all source nodes are able to transmit toward the sink directly (with a transmit power of $8W$), except for those at the corners of the deployment area. Source nodes located at the corners can transmit either to an adjacent sensor node on the bottom (needing $8W$) or to the nodes right above them (at 50 m depth). In this second case they spend $2W$ to transmit vertically, and then an additional $8W$ to advance the packet from there to the sink. This sums up to $8 + 2 = 10W$ which is less than what would be consumed following any alternative route to the sink (which would require at least $16W$). Since our schedule minimizes the total energy consumption, it always forces corner source nodes to send vertically to nodes which will deliver the packet directly to the sink. This routing strategy requires that four additional relays are placed at the four corners of the deployment area at 50 m.

The source node that is located in the center position on the bottom can either transmit directly to the sink (with a power of $8W$) or vertically one layer up to the central node at the depth of 50m (with power $2W$). Such node can relay the packet to the sink using a transmit power equal to $2W$. Traversing two vertical links is a better solution (with a total power consumption equal to $4W$) than any alternative route and it is therefore the route enforced by the model. This however demands for an additional relay node to be placed centrally at the depth of 50m.

Any other source node should transmit directly to the sink (with an associated transmit power equal to $8W$). When $p = 1$ this sums up to $76W$ needed for packet transmission and $10.5W$ spent for packet reception, resulting in an overall energy consumption of $86.5W$.²

As explained above, in addition to minimizing the total energy consumption we have also tried to decrease the time to deliver all packets, and also to limit the number of additional relay nodes. It is thus interesting to look at the average end-to-end latency performance to assess the effectiveness of our scheme in scheduling the

²Although it would be more physically correct to measure the energy consumption in Joules, we refer here for ease of explanation to the Watts of power, which are related to the energy consumption by a constant factor since packets are assumed to be of constant length.

generated traffic. The average end-to-end packet latency and the minimum time needed to deliver all the generated packets (schedule length T) are reported in Table 1. Note that a lower bound for T is given by the total number of generated packets $|S| \times p$ plus one propagation delay. In all cases considered, the total delay measured in our experiments is at most 100% larger than this minimum value. This additional time is due to the fact that, although the optimum schedule would ideally correspond to the sink continuously receiving packets, this is not always possible due to the need to maintain the interference constraints when scheduling concurrent transmissions, which is made especially challenging here by the long propagation delays. More importantly, the difference in the time needed to propagate packets over the different links requires a careful schedule to try to reduce the sink idle times while avoiding simultaneous receptions.

In order to provide some understanding of the principles followed by the optimum scheduling and routing schemes, we describe here in detail one specific solution of the model for the case where $p = 1$. The resulting packet scheduling is displayed in Figs. 2(a) to Fig. 2(d) An arrow between a node i and a node j means that a packet is transmitted by the sensor in node i to the sensor in node j . Each arrow is labeled with a number which is the time slot at which the packet transmission begins. Unlike in terrestrial wireless sensor networks, where the propagation delay is typically negligible, in the underwater environment two nodes x and y can transmit in the same slot to the same node z if the difference of the propagation delays over links (x, z) and (y, z) is more than one slot, since in this case the two packets do not overlap at the receiver. This is for example what happens in slot 12. Both node 4 and node 2 transmit one packet to the sink (node 18). However, the two packet receptions do not overlap, since the packet transmitted by node 4 reaches the sink after 0.17 slots (and its reception ends after 1.17 slots), while the packet transmitted by node 2 reaches the sink after 1.42 slots, after the first packet has been fully received. This is a basic difference with respect to traditional terrestrial WSN (due to the specific properties of underwater propagation) which has to be accounted for in designing protocols for underwater sensor networks.

The jointly optimized traffic scheduling and routing scheme derived by our model effectively exploits the possibility of transmitting in parallel multiple packets whenever possible (i.e., when the interference constraints allow it). Links in different parts of the networks are activated over time according to interference constraints. More importantly, the order of links activation/deactivation is properly selected to exploit the different link propagation delays, minimizing the idle time at all receivers (especially the sink), which results in improved efficiency and fast packet delivery.

Let us discuss in detail the schedule behavior. In slot 0 four parallel transmissions are performed, from the four corner source nodes vertically to the relay nodes placed just above them. Node 9 transmits to node 0, node 11 to node 2, node 15 to node 6 and node 17 to node 8. Concurrent packet transmissions occur even if the interference received from any corner source node would be enough to impair reception at one of the nodes on the upper layer. The trick for enabling parallel transmission is in the different signal propagation delays. The propagation of the messages transmitted by any other corner source node reaches node 0 when it has completely received the packet transmitted by node 9. This also explains why the packet generated by the central node cannot be scheduled in slot 0. If this were the case, a packet sent by node 13 would reach nodes 0, 2, 6, 8 while they are still receiving the packets generated by the corner source nodes. This would result in unsuccessful packet reception. The same reasoning apply to the packets generated by source nodes on the sides (nodes 10, 12, 14 and 16). No such nodes can transmit if all the corners links are activated. Nodes 10, 12, 14 and 16 transmit

at $8W$, resulting in even stronger interference than what would be caused by node 13, and are located too close to the adjacent corners to exploiting differences in propagation delays to achieve concurrent packet transmission.

A similar reasoning motivates why no node can transmit in slot 1 (even if we are trying to minimize the time to complete packet transmissions): this would interfere with the transmissions started in slot 0. In slot 2 transmissions from the upper layer to the sink start. Being nodes 0 and 6 symmetrically placed (except for the the random vertical/horizontal offset with respect to the grid position) their transmissions can be effectively scheduled one after the other so that packets are received at the sink with little or no inter-packet spacing. This is what is done in slots 2 and 3. A similar decision is made by the model for what concerns the transmissions from the almost symmetrical nodes placed at the sides of the bottom area. They are scheduled one after the other in slots 6 through 9. The order of the different link activations is not random. Links are activated from the one resulting in lower propagation delay to the one resulting in higher propagation delay, so that receptions can occur one after another at the sink, which tries to minimize the sink idle time.

As a final note the minimum number of sensors k placed by the model without degrading the energy consumption is 14. With fewer nodes some of the generated packets could not be transmitted over minimum energy routes, which would result in increased total energy consumption.

When the sink is located on the side of the deployment area (right above node 5), shortest path routes from the source to the sink are longer than in the case in which the sink is centrally placed. In this case nodes 11, 13, 17 transmit directly to the sink with $8W$. Packets generated by node 14 are more energy-efficiently delivered to the sink going through a 2-hop path which traverses node 5 (with an overall energy consumption of $4W$). Packets generated by all the other source nodes first have to advance toward the sink (either horizontally, or diagonally toward nodes 1, 4, 5, 7) with an energy consumption of $8W$, and then can be transmitted toward the sink (with an additional consumption of $8W$). The increased route lengths, and the fact that higher transmit powers have to be used in this case, translate into increased total energy consumption. The end-to-end latency also increases (since longer routes have to be traversed).

The optimal packet scheduling and routing is displayed in Figs. 3(a) to Fig. 3(d) Differently from terrestrial radio sensor networks, a node x could start transmitting in a given slot to node y , even though y is currently transmitting, if the packet sent by x will reach y after it has completed its current transmission. This occurs in slot 11. Even if node 13 starts transmitting to 18 in slot 11, it completes such transmission before starting reception of the packet generated by node 15, which reaches it after 1.41 time slots. Concurrent packet transmissions are performed whenever possible. In slot 14 nodes 13 and 5 transmit simultaneously to the sink (thanks to the different propagation delays, which result in non-overlapping packets reception at the sink). In slots 7 and 0 vertical non-interfering links are activated simultaneously.

An interesting kind of parallelism occurs also in the transmissions performed in slots 2 and 3. In slot 2 node 1 starts transmitting toward node 18. In slot 3 node 12 transmits to node 4. This second transmission could potentially be disturbed by the propagation of the acoustic wave emitted by node 1. However, such wave propagates beyond node 4 before node 4 starts receiving the message transmitted by node 12, resulting in no interference.

Even in this case activation of the links toward the sink is performed so as to minimize the sink idle time. This results in lower packet latencies.

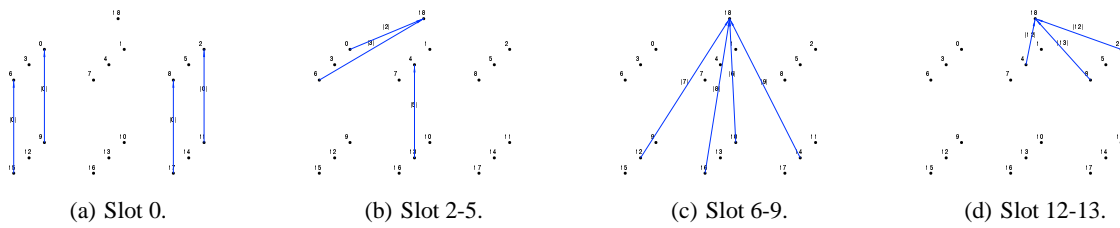


Figure 2: 3x3x2 schedule: $p = 3$, sink centrally placed.

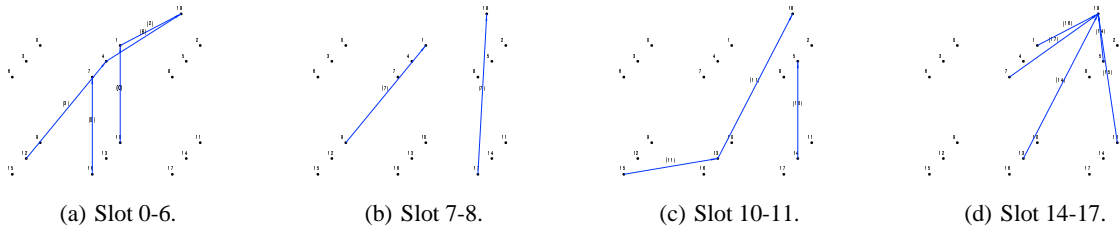


Figure 3: 3x3x2 schedule: $p = 3$, sink centrally placed.

6. CONCLUSIONS

We presented a novel optimization framework for joint sensor deployment, link scheduling and routing in underwater sensor networks. This model is able to capture the unique features of the underwater propagation environment, as well as interference conditions at each receiver. Validation has shown that our model is able to exploit specific features of the environment, such as the large differences in propagation delays over different links, etc. Our study led us to interesting observations about optimal scheduling and routing in UW sensor networks, which will result in novel protocol design and implementation criteria.

7. REFERENCES

- [1] AKYILDIZ, I. F., POMPILI, D., AND MELODIA, T. Underwater acoustic sensor networks: Research challenges. *Elsevier's Ad Hoc Networks* 3, 3 (May 2005), 257–279.
- [2] ALONSO, J., AND FALL, K. A linear programming formulation of flows over time with piecewise constant capacity and transit times. TR IRB-TR-03-007, Intel Research, 2003.
- [3] BHARDWAJ, M., AND CHANDRAKASAN, A. P. Bounding the lifetime of sensor networks via optimal role assignments. In *Proc. IEEE INFOCOM* (2002), vol. 3, pp. 1587–1596.
- [4] CHANG, J.-H., AND TASSIULAS, L. Maximum lifetime routing in wireless sensor networks. *IEEE/ACM ToN* 12, 4 (2004), 609–619.
- [5] CODIGA, D., RICE, J., AND BAXLEY, P. Networked acoustic modems for real-time data delivery from distributed subsurface instruments in the coastal ocean: Initial system development and performance. *J. Atmos. Oceanic Tech.* 21, 2 (2004), 331–346.
- [6] GNU. *glpk 4.8*, 2006. <http://www.gnu.org/software/glpk/>.
- [7] GUPTA, P., AND KUMAR, P. R. The capacity of wireless networks. *IEEE Trans. on Information Theory* 46, 2 (2000).
- [8] JAIN, K., PADHYE, J., PADMANABHAN, V. N., AND QIU, L. Impact of interference on multi-hop wireless network performance. In *Proc. ACM Mobicom* (2003), pp. 66–80.
- [9] KODIALAM, M., AND NANDAGOPAL, T. Characterizing achievable rates in multi-hop wireless networks: the joint routing and scheduling problem. In *Proc. ACM Mobicom* (2003), pp. 42–54.
- [10] KODIALAM, M., AND NANDAGOPAL, T. Characterizing the capacity region in multi-radio multi-channel wireless mesh networks. In *Proc. ACM Mobicom* (2005), pp. 73–87.
- [11] KOTNYEK, B. An annotated overview of dynamic network flows. TR RR-4936, INRIA, 2003.
- [12] KUMAR, V. S. A., MARATHE, M. V., PARTHASARATHY, S., AND SRINIVASAN, A. Algorithmic aspects of capacity in wireless networks. In *Proc. ACM SIGMETRICS* (2005), pp. 133–144.
- [13] LINDSEY, S., RAGHAVENDRA, C., AND SIVALINGAM, K. M. Data gathering algorithms in sensor networks using energy metrics. *IEEE TPDS* 13, 9 (Sept. 2002), 924–935.
- [14] LINKQUEST INC. *Underwater acoustic modems data sheets*. Last accessed on July 2006 at http://www.link-quest.com/html/uwm_hr.pdf.
- [15] MADAN, R., AND LALL, S. Distributed algorithms for maximum lifetime routing in wireless sensor networks. In *Proc. IEEE Globecom* (2004), pp. 748–753.
- [16] MARINA, M. K., AND DAS, S. R. A topology control approach for utilizing multiple channels in multi-radio wireless mesh networks. In *Proc. Broadnets Symposium* (2005).
- [17] SINGH, S., WOO, M., AND RAGHAVENDRA, C. S. Power-aware routing in mobile ad hoc networks. In *Proc. ACM/IEEE Mobicom* (1998), pp. 181–190.
- [18] SOZER, E. M., STOJANOVIC, M., AND PROAKIS, J. G. Underwater acoustic networks. *IEEE Journal of Oceanic Engineering* 25 (2000), 72–83.
- [19] URICK, R. J. *Principles of Underwater Sound*. McGraw-Hill, 1983.
- [20] WATTENHOFER, R., LI, L., BAHL, P., AND WANG, Y.-M. Distributed topology control for power efficient operation in multihop wireless ad hoc networks. In *Proc. ACM/IEEE INFOCOM* (2001).
- [21] YU, Y., KRISHNAMACHARI, B., AND PRASANNA, V. K. Energy-latency tradeoffs for data gathering in wireless sensor networks. In *Proc. IEEE INFOCOM* (2004), vol. 1.